NEW MESOPOROUS MATERIALS WITH SURFACE SUPRAMOLECULAR CENTRES FOR METHYL RED SORPTION

Nadiia Roik [*], Lyudmila Belyakova, Marina Dziazko, Iryna Trofymchuk

Chuiko Institute of Surface Chemistry of NAS of Ukraine, 17, General Naumov str., Kyiv 03164, Ukraine
[*]*e-mail: roik_nadya@ukr.net; phone: (+380) 44 422 96 91; fax: (+380) 44 424 35 67*

Abstract. Macrocyclic units were introduced into the surface layer of mesoporous silica by sol-gel condensation of tetraethyl orthosilicate and β-cyclodextrin-containing silane in water-ammonium solution in the presence of a structure directing agent. Chemical and porous structure of parent and β-cyclodextrin-containing silica materials were elucidated by IR spectral and chemical analysis of surface functional groups, as well as nitrogen adsorption-desorption isotherms, X-ray diffraction, transmission electron microscopy and dynamic light scattering. It was found that the incorporation of cyclic oligosaccharide moieties into the hexagonally arranged mesoporous framework leads to the enhancement of sorption efficiency towards methyl red. Adsorption of dye from phosphate buffer solutions was studied as function of pH, contact time and methyl red concentration. Obtained results of equilibrium sorption were analyzed using Langmuir, Freundlich, Redlich-Peterson, Dubinin-Radushkevich and Brunauer-Emmet-Teller isotherm models.

Introduction

Cyclodextrins (CDs) are cyclic oligosaccharides consisting of glucopyranose units linked by α-1,4 glycosidic bonds. Due to their unique structure, CDs are able to form inclusion complexes with various organic molecules in aqueous solutions. Binding ability, which characterizes the strength of host-guest molecular interaction, is driven by non-covalent forces and depends mostly on geometrical parameters [1,2]. The ability of CDs to selectively include some molecules into the hydrophobic cavity can be useful in separation processes [3]. However, the extraction of supramolecular complexes from aqueous solutions is complicated by their high solubility. This problem can be solved by immobilization of CDs on the surface of water insoluble materials.

The macrocyclic molecules bonded to silica can be considered as potential carriers or sorbents of organic substances [4,5]. Well-defined surface properties of silica and the presence of highly reactive silanol groups allow easy directed functionalization of its surface with CD moieties. Introduction of oligosaccharide macromolecules into the silica matrix can be accomplished by co-condensation of functional silanes [6-9] or by postsynthetic modification procedure [10-18].

Mesoporous silica materials with chemically immobilized CDs combine the advantages of inorganic framework, such as favourable chemical properties, high thermal stability, biocompatibility, nontoxicity, and the ability of CDs to form various inclusion complexes with a wide range of organic molecules. Of particular importance are the organosilica materials of MCM-41-type containing cyclic oligosaccharides on the surface of regular pore channels, due to their high surface area and accessibility of sorption centres [7,8,10,18].

In this paper, a simple strategy for the synthesis of β-CD-containing silica with hexagonally ordered mesoporous structure was proposed. In the first step, chemical modification of β-CD was performed using (3-aminopropyl)triethoxysilane (APTES) and 1,1'-carbonyldiimidazole (CDI) as coupling agent. As a result, highly reactive triethoxysilyl groups were introduced into the structure of macrocyclic oligosaccharide. Further, the synthesized β-CD-containing silane was involved into the co-condensation reaction with tetraethyl orthosilicate (TEOS) in the presence of template quaternary alkylammonium ionic surfactant. It was supposed that the organosilica material with hexagonally arranged uniform mesoporosity, providing

improved access of "guest" molecules to the macrocyclic binding sites, can be useful in the sorption and removal of aromatic compounds, in particular dyes from water solutions. In the present work, the sorption of methyl red (MR) by parent MCM-41 and by synthesized *β*-CD-containing silica has been studied as function of the pH of the solution and equilibrium concentration of the dye in phosphate buffer solutions. The obtained results were analyzed using several isotherm models and the most appropriate one was chosen for each isotherm based on error analysis.

Experimental
Materials

Tetraethyl orthosilicate (from Merck, purity ≥99%), cetyltrimethylammonium bromide (CTMAB) (from Merck, purity ≥97%), *β*-cyclodextrin (from Fluka, purity ≥99%), (3-aminopropyl)triethoxysilane (from Merck, purity ≥99%), 1,1'-carbonyldiimidazole (from Merck, purity ≥98%), methyl red sodium salt, disubstituted sodium phosphate and monosubstituted potassium phosphate (all from Reakhim, pure analytical), hydrochloric acid 37% and ethanol 96% (all from Reakhim, chemical grade) were used without additional purification. N,N′-dimethylformamide (DMF) (from Reakhim, pure analytical) was dried for 72 h by use of 4 Å molecular sieves. All other chemicals used in this study were of analytical grade.

Synthesis of MCM-41 silica

The MCM-41 silica material was synthesized by base catalyzed sol-gel condensation of tetraethyl orthosilicate (TEOS) in the presence of quaternary ammonium salt as structure directing agent [19]. The precipitated white product was kept in the reaction mixture and stirred for 2 h, then transferred to a polypropylene bottle and hydrothermally treated at 373 K for 24 h. After that, the synthesized silica was filtered, washed with 100 mL of deionized water and air dried at 373 K for 3 h.

Extraction of CTMAB from the mesoporous volume of MCM-41 was achieved by stirring the batch of the synthesized silica (1 g) with a solution of hydrochloric acid (8 mL) and ethanol (92 mL) at 298 K for 24 h. After separation of silica particles from solution by filtration, the extraction procedure was repeated two more times. The resulting mesoporous silica was filtered, washed with deionized water until the absence of halogen ions in the filtrate (negative probe with silver nitrate), and air dried at 373 K for 5 h.

Synthesis of β-CD-containing silane

β-CD-containing silane was prepared from the parent *β*-CD and (3-aminopropyl)-triethoxysilane (APTES) by standard coupling procedure [20] widely used in the synthesis of functional silanes for subsequent sol-gel condensation or postsynthetic modification of silica [21-24]. The batch of *β*-CD (0.001 mol) was dissolved in 15 mL DMF and treated with 1,1'-carbonyldiimidazole (CDI) solution (0.003151 mol) in DMF. Since CDI is highly sensitive to moisture, its excess (5%) was added to the reaction solution, related to the calculated triple molar excess. To complete the activation of oligosaccharide hydroxyl groups, the reaction mixture was stirred at 293 K for 2 h. Then APTES (0.003 mol) was added into the reaction flask to link with activated *β*-CD. The solution was stirred at 293 K for 20 h and used in sol-gel synthesis of the corresponding *β*-CD-containing silica material.

Synthesis of β-CD-containing silica

The *β*-CD-containing mesoporous material of MCM-41-type was synthesized according to the procedure described previously [25,26]. Briefly, a weighted amount of CTMAB (0.0069 mol) was dissolved under vigorous stirring in distilled water (7.2 mol), followed by the addition of 25% aqueous ammonium (0.27 mol). Further, TEOS (0.049 mol) was added to the obtained mixture under continuous stirring at 293 K. The reaction slurry was agitated at 293 K for 2 h, transferred into a polypropylene bottle and heated at 373 K for 24 h. The solid precipitated product was filtered, rinsed with deionized water and air-dried at 373 K for 2 h.

Extraction of the surfactant template from pore channels of mesoporous organosilica was done in acid-ethanol medium as described above. Organosilica material obtained using *β*-CD-containing silane was noted as *β*-CD-MCM-41.

Characterization methods

Porous structure characterization of silica materials was performed using data of low-temperature (77 K) nitrogen adsorption-desorption isotherms obtained with a Kelvin-1042 Sorptometer. Firstly, silica was outgassed under vacuum at 413 K for 20 h and then analyzed in the region of relative pressures from 0.06 to 0.99. Specific surface area was evaluated by Brunauer-Emmet-Teller (S_{BET}) method and pores diameter was calculated by density functional theory (DFT). Pores volume was determined at $p/p_o = 0.99$.

X-ray diffraction spectra were registered using the DRON-4-02 diffractometer with

monochromatic CuKα emission (λ= 0.15418 nm) and nickel filter. Interplanar distances were calculated using Bragg diffraction equation [27]. The unit cell parameters were calculated as in the literature [28].

Hydrodynamic size of silica particles was evaluated by dynamic light scattering (DLS) using Malvern Zetasizer (Version 7.11). All measurements were performed for diluted aqueous suspensions of synthesized silica materials (0.1 mg/mL) and repeated eight times at 278 K.

The transmission electron microscopy (TEM) images of mesoporous silicas were registered on a JEM-100CXII electron microscope at 200 kV. Carbon-coated copper grids were used as silica holders.

Chemical structure of synthesized mesoporous silica was confirmed by IR spectra recorded at room temperature using a Thermo Nicollet NEXUS FT-IR spectrophotometer in the frequency range from 4000 to 1200 cm^{-1} with a resolution of 2 cm^{-1}.

The content of β-CD moieties introduced into the silica during the sol-gel synthesis was estimated by acid hydrolysis of surface β-CD-containing groups to glucose and their subsequent determination by colour reaction with potassium ferricyanide. For this, a batch of silica (0.1 g) was refluxed with 15 mL of 1 mol/L sulphuric acid at 373 K for 2 h. Then the solution was neutralized with 5 mol/L sodium hydroxide up to pH 7; filtered and diluted with water up to 50 mL. A volume of 2 mL of the prepared solution was mixed with 25 mL of 0.05% potassium ferricyanide dissolved in 1% sodium carbonate water solution and boiled at 373 K for 10 min. After cooling, the concentration of glucose was determined colorimetrically with potassium ferricyanide at λ_{420} [29]. The glucose calibration curve was plotted over the range 0-160 µg/mL. The content of grafted β-CD was calculated by Eq.(1):

$$[\beta\text{-CD}] = \frac{C \cdot V}{7 \cdot m} \qquad (1)$$

where, [β-CD]- content of β-CD on the silica surface, mol/g;
C- concentration of glucose in the solution, mol/L;
V- volume of solution, L;
m- batch of β-CD-containing silica, g.

The concentration of 3-aminopropyl groups of β-CD-containing silica was determined by pH-metric method [30]; the batches of silica materials (0.5 g) were stirred with 25 mL of 0.01 mol/L hydrochloric acid in 50 mL round bottom glass flasks at 293 K for 24 h to attain equilibrium. The pH values of starting and equilibrium solutions were measured using the I-120.1 Ionometer that was calibrated with standard buffer solutions of pH 1.68 and pH 6.86 for optimal precision. The content of 3-aminopropyl groups chemically immobilized on the surface of mesoporous silica particles was calculated by Eq.(2):

$$[NH_2] = \frac{(10^{-pH_1} - 10^{-pH_2}) \cdot V}{m} \qquad (2)$$

where, [NH$_2$]- content of 3-aminopropyl groups of mesoporous silica, mol/g;
pH$_1$ and pH$_2$- pH of starting and equilibrium solutions, respectively;
V- volume of solution, L;
m- weight of mesoporous silica batch , g.

UV-Vis spectra of MR buffer solutions were recorded in 200-600 nm spectral range with a Specord M-40. Quarts cells with 2 mm path length were used. All spectroscopic measurements were performed in a temperature-controlled cell holder and water bath.

Distribution diagrams of protolytic forms of MR as well as silanol and 3-aminopropyl groups on silica surface were generated for the parameter set chosen in each simulation by the CURTIPOT program version 3.5.4.

Sorption of methyl red on MCM-41 and β-CD-MCM-41 silica

Sorption kinetic experiment

In a kinetic experiment, a series of MCM-41 or β-CD-containing silica batches of 0.01 g were placed in 50 mL glass beakers and 10 mL of 0.1336 mmol/L MR solutions in phosphate buffer with pH 1.0 or 7.0 were added. After shaking the prepared suspensions at 293 K, varying the contact time, the concentration of MR was determined in aliquots by measuring the optical density at λ_{523} or λ_{432}, respectively, using the UV-Vis Specord M-40 spectrophotometer.

The amount of MR sorbed on silica surface at time *t* was calculated by Eq.(3):

$$A_t = \frac{(C_o - C_t) \cdot V}{m \cdot S_{BET}} \cdot 1000 \qquad (3)$$

where, A_t- content of MR sorbed on silica surface at time *t*, µmol/g;
C_o and C_t- concentrations of MR at the initial moment and at time *t*, correspondingly, mmol/L;

V- volume of solution, L;
S_{BET}- specific surface area, m²/g;
m- weight of sorbent used, g.

pH-dependent sorption studies

Sorption of MR on MCM-41 and *β*-CD-MCM-41 silica as a function of pH was carried out using phosphate buffer solutions (0.02 and 0.0668 mmol/L). Samples of 0.01 g of silica and 10 mL of MR phosphate buffer solutions with predetermined pH ranging from 1.0 to 8.0 were placed in 50 mL glass beakers and shaken at 293 K for equilibrium attainment. Then supernatant solutions were separated by filtering through a 0.22 μm PVDF syringe filter and MR concentration was determined by a UV-Vis spectrophotometer (in the range of λ_{530} - λ_{424}).
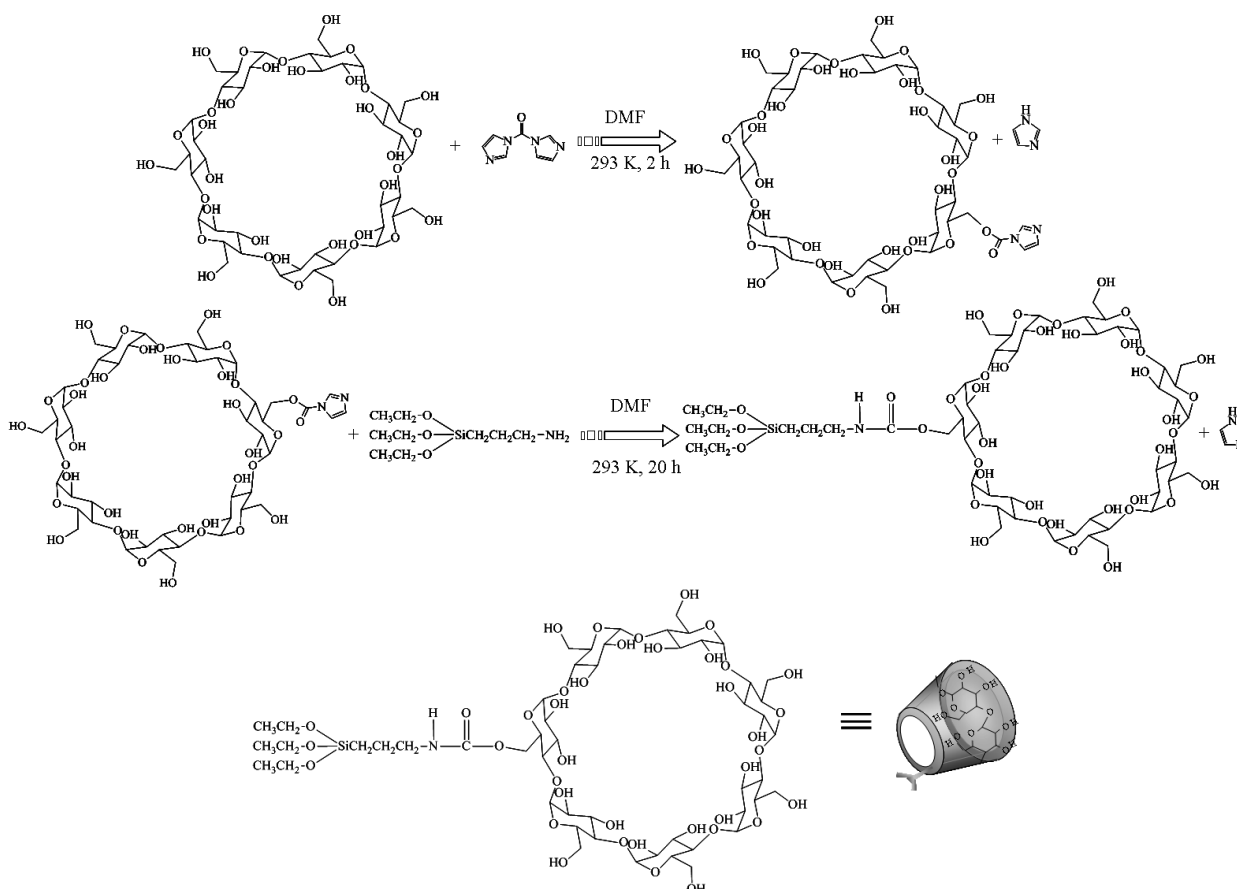
Sorption equilibrium experiment

Sorption equilibrium studies were performed by multibatch method; samples of 0.01 g of MCM-41 and *β*-CD-MCM-41 silica and 10 mL of MR phosphate buffer solutions with pH 1.0 or 7.0 and a predetermined concentration of dye in the range of 0.03717-0.3717 or 0.0167-0.167 mmol/L, correspondingly, were placed in 50 mL glass beakers and shaken at 293 K for equilibrium attainment. Then supernatant solutions were separated by filtering through a 0.22 μm PVDF syringe filter and MR concentration was determined at λ_{523} or λ_{432} for pH 1.0 or 7.0, correspondingly.
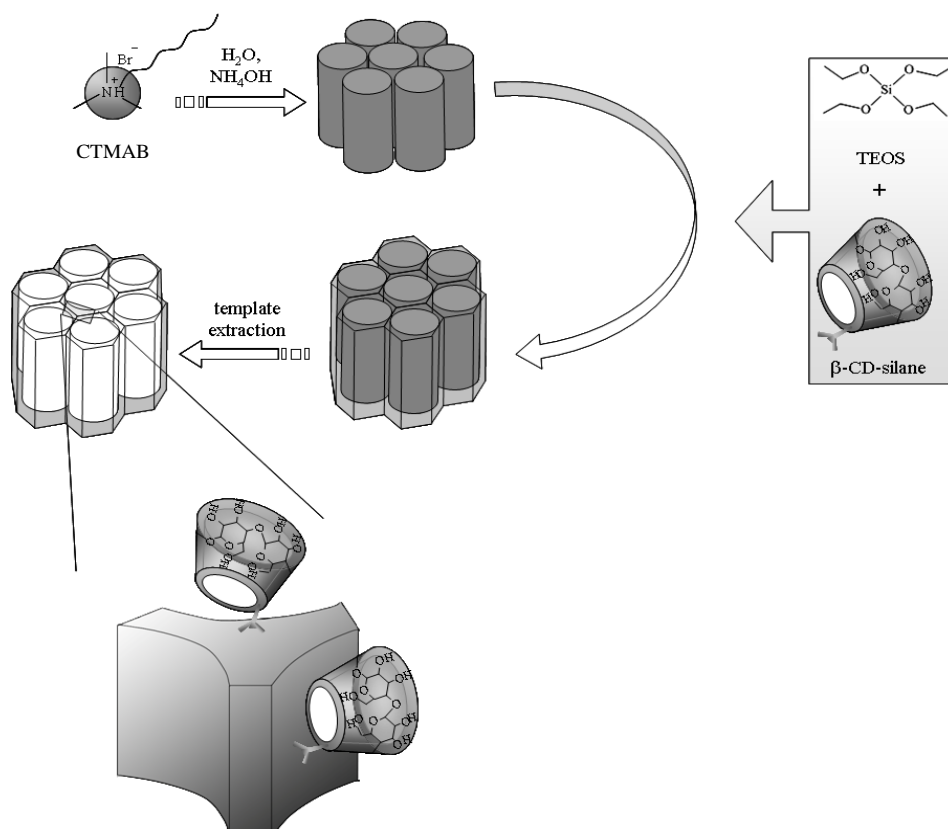
Results and discussion

Chemical composition and porous structure of synthesized silica materials

To provide homogeneous allocation of *β*-CD-containing groups on the surface of mesoporous silica, sol-gel condensation of TEOS and *β*-CD-silane was realized in water-ammonium solution in the presence of structure-directing agent (alkyltrimethylammonium salt). APTES was employed in the present work to introduce highly reactive alkoxy groups in the structure of *β*-CD activated with 1,1'-carbonyldiimidazole (Scheme 1) for subsequent immobilization of cyclic oligosaccharide moieties into the silica framework (Scheme 2).

Scheme 1. Activation of *β*-CD with 1,1'-carbonyldiimidazole and its coupling with APTES.

Scheme 2. Synthetic route for *β*-CD macromolecules introduction into the silica structure.

The incorporation of *β*-CD moieties into the silica structure was evidenced by IR spectral studies and chemical analysis of surface layer of synthesized materials. The IR spectra of *β*-CD-MCM-41 shows the absorption bands at 3000-2500 cm^{-1} corresponding to the valence vibrations of the C-H bonds of immobilized *β*-CD-containing silane (Figure 1). The most noticeable among them is a strong characteristic band at 2938 cm^{-1} assigned to the valence vibrations of the C-H bonds in the CH and CH$_2$ groups of *β*-CD rings. The peaks attributed to the valence vibrations of the C=O bond in the carbonyl groups and the deformation vibrations of the N-H bond in the secondary amino groups are registered at 1697 and 1540 cm^{-1}, respectively. Their appearance in the IR spectra of *β*-CD-MCM-41 proves the successful introduction of oligosaccharide groups into the silica framework (Scheme 1).

According to the chemical analysis data, the hydrolysis of a certain number of amide bonds in *β*-CD-silane during sol-gel synthesis of silica functional material in the presence of aqueous ammonium causes the appearance of primary amino groups in the structure of resulting *β*-CD-MCM-41. However, their identification in the IR spectrum of synthesized material is complicated, because of the overlapping of the characteristic absorption bands generated by the deformation vibrations of N-H bonds in primary and secondary amino groups.
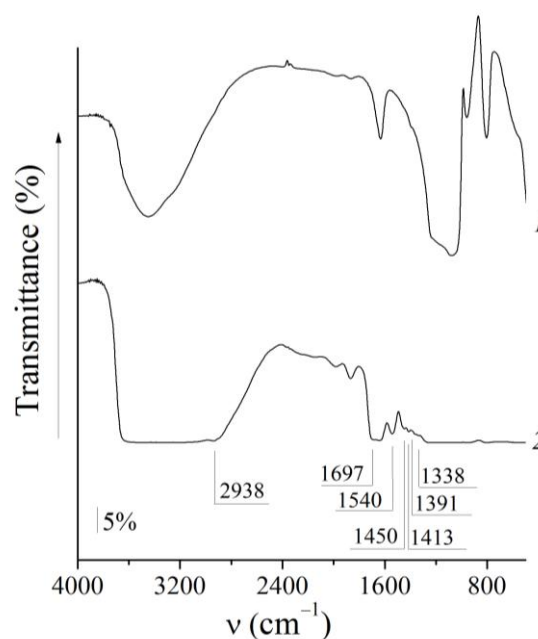

Figure 1. IR spectra of MCM-41 (*1*) and *β*-CD-MCM-41 (*2*).

The band at the lower frequencies with a maximum at 1450 cm^{-1} is assigned to the bending vibrations of C-H, H-C-H and C-O-H bonds in alkyl and glycosyl groups of grafted compounds [31], whereas the bands at 1413 and 1391 cm^{-1} belong to the bending vibrations of C−C–H and C-O-H bonds in the same groups, correspondingly. In the IR spectrum of *β*-CD-MCM-41 an additional absorption band is registered at 1338 cm^{-1}. Its appearance is mainly attributed to the stretching vibrations of C-O and the bending vibrations of C-O-H bonds in *β*-CD-containing groups. The IR spectra indicate the successful chemical immobilization of *β*-CD macromolecules along with aminopropyl moieties on the silica surface providing multifunctional surface formation.

The content of cyclic oligosaccharide on the surface layer of synthesized organosilica determined by acid hydrolysis of *β*-CD to glucose [29] consists of 0.07 mmol/g, whereas the quantity of grafted aminopropyl groups determined by pH-metric method is equal to 0.11 mmol/g.

X-ray diffraction patterns of MCM-41-type silica are represented in Figure 2. The MCM-41 diffractogram shows three well-defined (100), (110) and (200) reflections characteristic for a hexagonally arranged porous structure. The peak intensity of the reflection from the (100) plane is over 14000 cps proving the higher ordered hexagonal arrangement of mesopore channels. Introduction of *β*-CD-silane into the sol-gel synthesis leads to the formation of silica material which is characterized by the less distinct long-range ordering of porous structure.
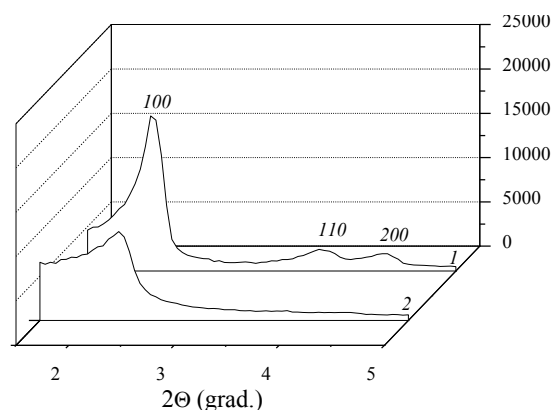

Figure 2. X-ray diffraction patterns of MCM-41 *(1)* and *β*-CD-MCM-41 *(2)*.

Figure 2 clearly shows that the intensity of the diffraction peak corresponding to the (100) reflection decreases in the case of *β*-CD-MCM-41. At the same time, high-angle diffraction peaks are not registered in the diffractogram of *β*-CD-MCM-41.

The structural parameters of synthesized silica materials (MCM-41 and *β*-CD-MCM-41) were determined from nitrogen adsorption-desorption isotherms (Figure 3). A sharp increase in nitrogen adsorption observed at low relative pressures (<0.3) on the isotherms of MCM-41 and *β*-CD-MCM-41 can be attributed to the monolayer adsorption in mesopores. Specific surface areas calculated for this interval of relative pressures using BET method [32] are represented in Table 1.
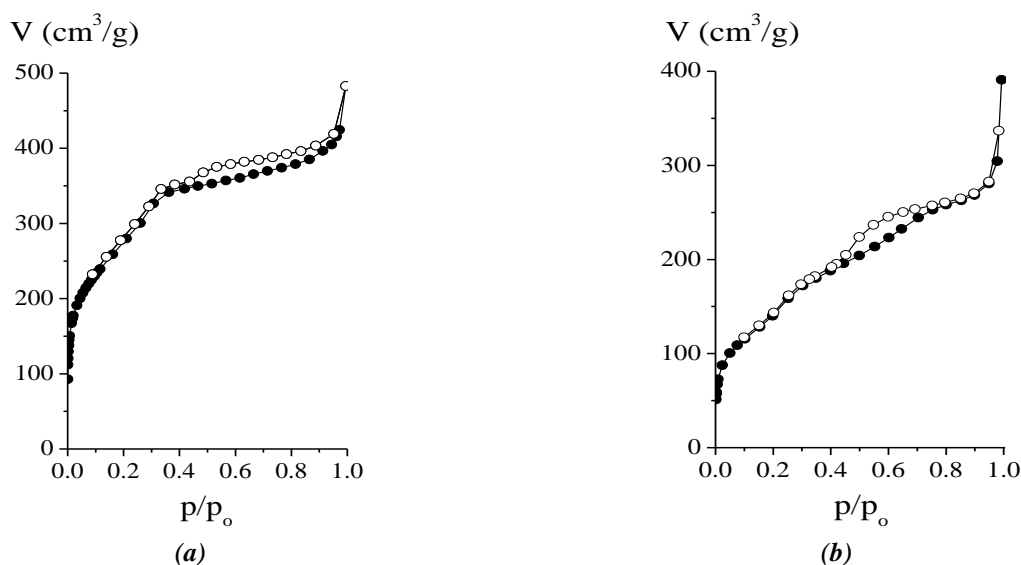

Figure 3. Nitrogen adsorption-desorption isotherms for MCM-41 *(a)* and *β*-CD-MCM-41 *(b)*.

The hysteresis loop on the isotherm of MCM-41 observed at relative pressures above 0.3 is due to the capillary condensation of nitrogen inside the mesopores with narrow size distribution. The pore size distributions determined using the DFT theory, clearly demonstrates that mesopores with diameters less than 5.1 nm are prevailing in the synthesized materials (Figure 4, Table 1). Introduction of β-CD-silane into the sol-gel synthesis is accompanied by noticeable decrease of surface area of resulting silica (Table 1).

TEM was used to visualize the hexagonally arranged mesoporous structure of synthesized silica. Figure 5 shows that MCM-41 silica particles are rod-like shaped. Their size varies in the range from 1.5 to 2 μm (Figure 5(a)). The TEM image of β-CD-MCM-41 shows spherical particles with an average diameter of up to 400 nm and highly ordered hexagonal long-range array of channels (Figure 5(b)). Pore channels of MCM-41 as well as β-CD-MCM-41 are parallel to the horizontal particle axis and their entrances are accessible for an adsorbate (Figure 5).

Table 1

Structural parameters of mesoporous silicas calculated from nitrogen adsorption-desorption isotherms.

Silica	d_{100}, nm	a, nm	S_{BET}, m^2/g	V, cm^3/g	D, nm
MCM-41	4.17	4.82	995	0.75	3.7; 5.1
β-CD-MCM-41	3.93	4.54	512	0.60	2.5; 3.3; 5.1

(a)   *(b)*

Figure 4. Pore size distribution for MCM-41 *(a)* and *β*-CD-MCM-41 *(b)*.
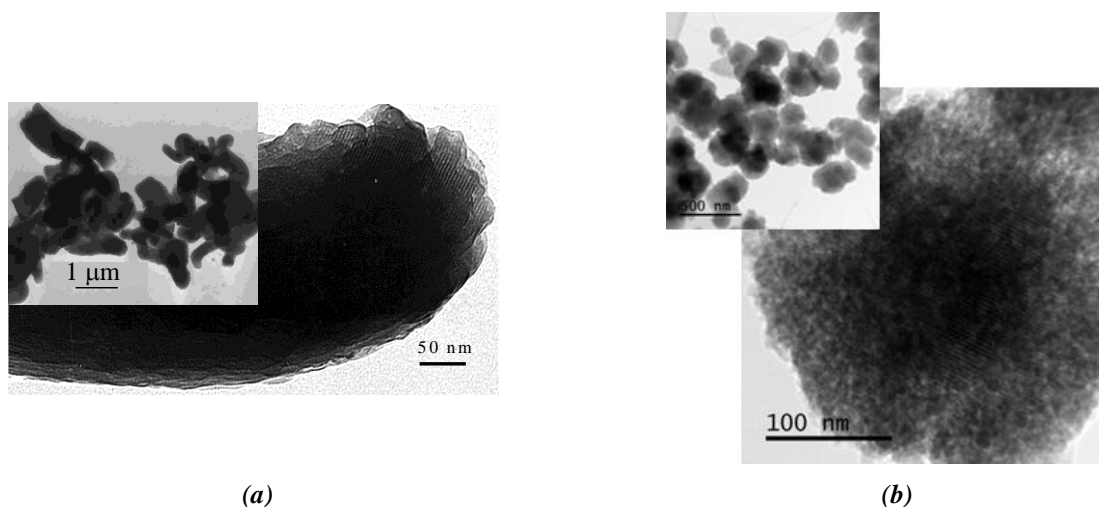

(a)   *(b)*

Figure 5. TEM images of MCM-41 *(a)* and *β*-CD-MCM-41 *(b)*.

The average size of *β*-CD-containing silica particles was determined from DLS measurements. It was found that mean hydrodynamic diameter of *β*-CD-MCM-41 particles calculated from the size distribution profiles was 714 nm (Figure 6). Relatively larger diameters calculated from DLS experiment in comparison with TEM results were due to the hydrated layer surrounding the particles with a narrow particle size distribution.
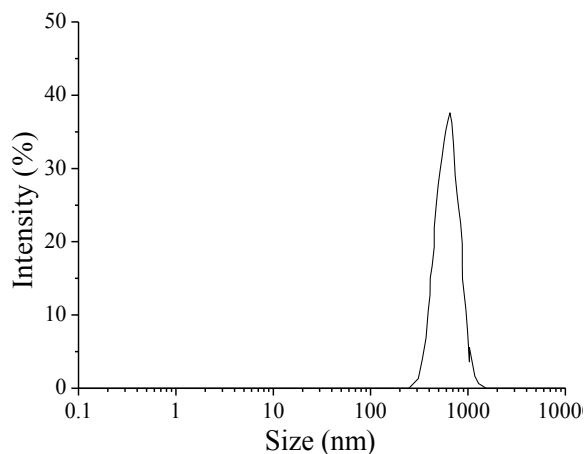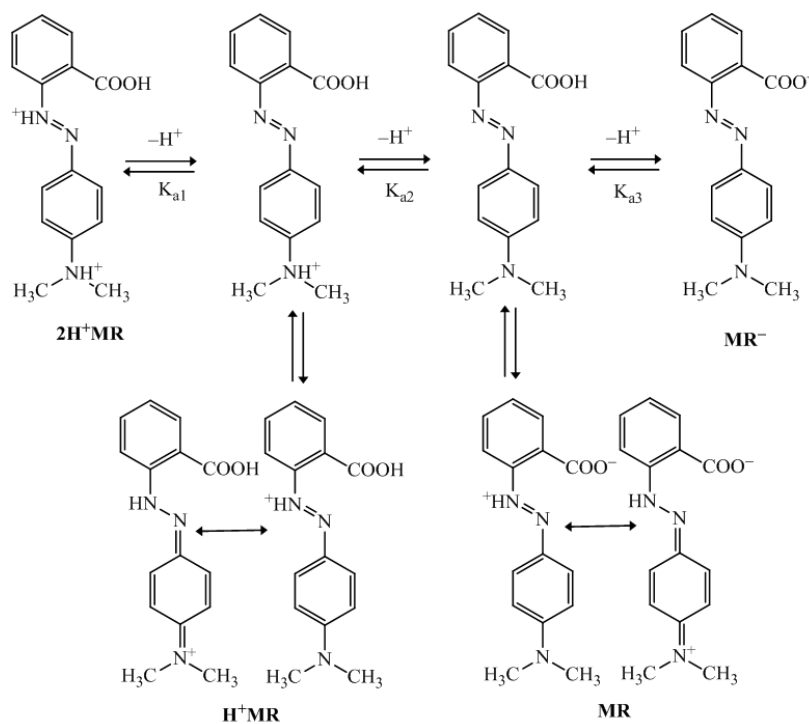

Figure 6. Particle size distribution of
***β*-CD-MCM-41.**

Sorption of methyl red on MCM-41 and
β-*CD-MCM-41 silica*

Adsorption capacity of both acid and basic dyes on initial MCM-41 is very low [33,34]. Therefore, surface functionalization of mesoporous silica was undertaken to enhance their affinity to various types of dyes [35-38]. To elucidate the contribution of macrocyclic surface centres to the removal of dye molecules from aqueous solutions, sorption of MR was studied on parent MCM-41 and chemically modified *β*-CD-MCM-41. Thereafter, obtained results were analyzed applying the most widely used kinetic and equilibrium sorption models and compared.

The pH value influences the MR sorption on MCM-41 and *β*-CD-MCM-41, because of the changes that are induced in the protolytic forms of dye molecules as well as on the silica surface. Under experimental conditions, MR has a complex acid-base equilibrium (Scheme 3). Ionized and several protonated forms of dye can exist in the pH range from 1 to 8 (Scheme 3, Figure 7) [39]. The value of pK_{a2} is 2.38±0.05 at 298 K [39], whereas pK_{a3} varies from 4.85±0.01 to 5.05±0.05 in the temperature range of 298-303 K [39-41].

Scheme 3. Protolytic species of methyl red.

The profile of Figure 8 indicates that the efficiency of MR sorption on MCM-41 and β-CD-MCM-41 improves with the increase of pH, attaining a maximal value in the pH range from 3 to 5. Obviously, hydrogen bonds formation between non-ionized silanol groups of MCM-41 and basic centres of MR (nitrogen of azo linkage and dimethylamino group) plays the key role in the sorption process (Figure 7). Likewise, removing of MR by β-CD-MCM-41 from weakly acidic aqueous solutions is most probably induced by hydrogen bonding with participation of silanol and 3-aminopropyl surface groups. Moreover, oligosaccharide macromolecules localized on the surface layer of β-CD-MCM-41 may contribute to dye sorption.

Kinetic studies of MR removal from acidic and neutral phosphate buffer solutions by parent and β-CD-functionalized mesoporous silica demonstrated that, regardless of the nature of functional groups on the surface of silica materials, equilibrium of dye sorption is achieved after 6 h of contact (Figure 9).
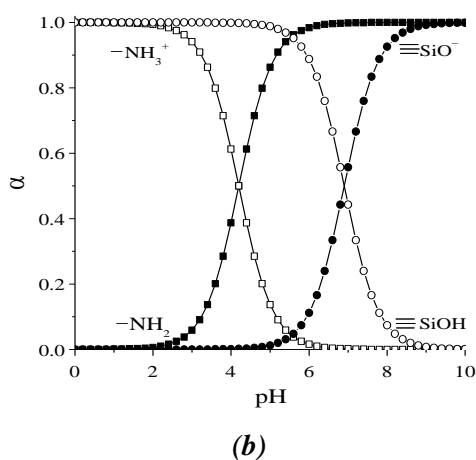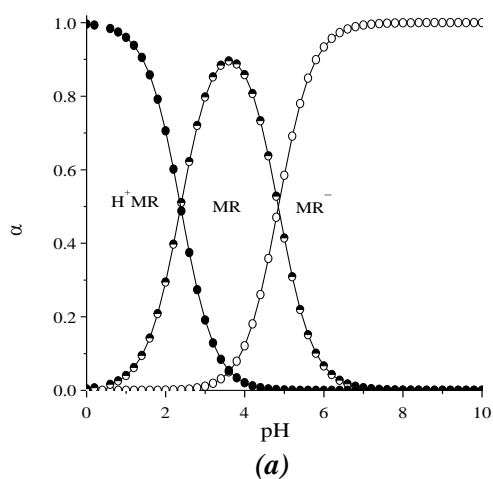
(a)

(b)

Figure 8. Effect of pH on MR sorption on MCM-41 *(1)* and β-CD-MCM-41 *(2)* silica from 0.02 mmol/L *(a)* and 0.0668 mmol/L *(b)* phosphate buffer solutions at 293 K.

(a)

(b)

Figure 7. Distribution diagrams of protolytic forms of MR *(a)* as well as surface silanol and 3-aminopropyl groups of silica materials *(b)* as a function of pH value.
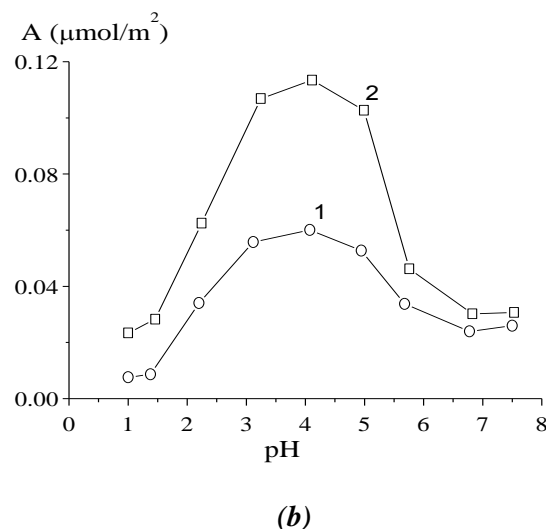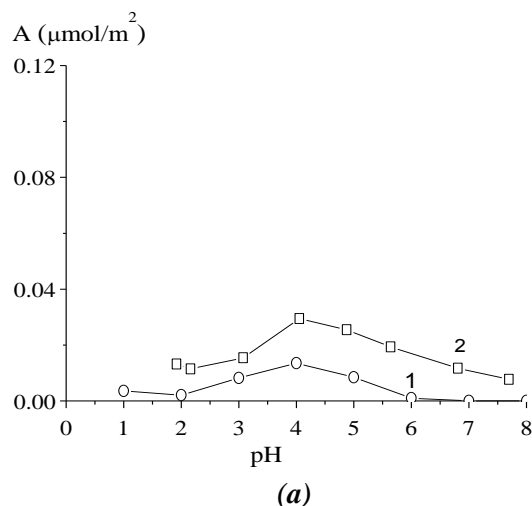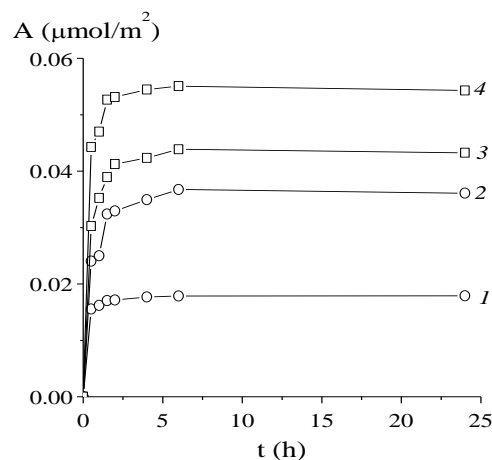
Figure 9. Kinetic curves of MR sorption on MCM-41 (circles) and β-CD-MCM-41 (squares) silica from phosphate buffer solutions (0.1336 mmol/L) with pH 1.0 (curves *1, 3*) and pH 7.0 (curves *2, 4*) at 293 K.

Analysis of kinetic curves was realized using pseudo-first and pseudo-second order kinetic equations of Lagergren and Ho-McKay, correspondingly (Table 2). Comparison of the correlation coefficients R^2, reflecting the agreement of experimental results and the model predicted values, proves that the kinetics of MR sorption on MCM-41 and β-CD-MCM-41 silica in acidic and neutral phosphate buffer medium can be successfully described by the Lagergren equation. At the same time, correlation coefficients calculated for the linear plots using pseudo-second order model are less than 0.715, whereas theoretical values of A_{eq} significantly exceed the experimental ones (Table 2). This leads to the conclusion that the sorption process of MR on synthesized materials follows the pseudo-first order kinetic model.

Table 2

Kinetic parameters for methyl red sorption on MCM-41 and β-CD-MCM-41 silica.

Kinetic adsorption model	Kinetic parameters	pH 1.0		pH 7.0	
		MCM-41	β-CD-MCM-41	MCM-41	β-CD-MCM-41
Lagergren	k_1 (1/min)	0.816	1.336	0.666	1.944
$lg\left(\dfrac{A_{eq}}{A_{eq}-A_t}\right)=\dfrac{k_1}{2.303}t$	A_{eq} (μmol/m^2)	0.005	0.041	0.020	0.065
	R^2	0.889	0.892	0.934	0.873
$lg\left(A_{eq}-A_t\right)=lgA_{eq}-\dfrac{k_1}{2.303}t$					
Ho-McKay	k_2 (m^2/(μmol·min))	0.026	0.067	0.137	0.020
$\dfrac{1}{\left(A_{eq}-A_t\right)}=\dfrac{1}{A_{eq}}+k_2t$	A_{eq} (μmol/m^2)	0.781	0.709	0.433	1.531
	R^2	0.715	0.599	0.633	0.579
$\dfrac{t}{A_t}=\dfrac{1}{k_2A_{eq}^2}+\dfrac{1}{A_{eq}}t$					

The sorption of MR on β-CD-MCM-41 was performed at pH values of 1.0 and 7.0 aiming to elucidate the role of β-CD-containing groups on dye removal from aqueous solutions. In acidic solutions MR exists in the H$^+$MR protolytic form, which is unable to form hydrogen bonds with protonated aminopropyl and nonionized silanol groups of silica surface (Scheme 3, Figure 7). In a neutral aqueous medium, the dye anion does not interact with aminopropyl groups having an unshared electron pair on the nitrogen atom, nor with the negatively charged ionized silanol groups (Scheme 3, Figure 7). Thus, the difference in adsorption of MR on MCM-41 and β-CD-MCM-41 at pH 1.0 and 7.0 can be mainly attributed to the presence of surface cyclic oligosaccharide groups, which are able to form inclusion complexes with protolytic forms of the dye. The obtained isotherms have different shapes depending on the nature of interactions between MR and functional groups on the silica surface (Figure 10). In particular, the dye sorption on β-CD-MCM-41 from acidic and neutral solutions can be attributed in accordance with the IUPAC classification to the type II, proving the interaction of the sorbate molecules with the higher energetic region followed by the interaction with the less energetic ones (Figure 10). The incorporation of β-CD macrocycles into the surface layer of MCM-41 leads to an increase in the sorption ability at least twice for the protonated form of dye H$^+$MR and for the MR$^-$ anion (Figure 10).

The equilibrium sorption data were analyzed to elucidate the mechanism of MR distribution between the liquid phase and silica sorbent and to optimize the design of a sorption system for dye removal, using widely applied isotherm models: Langmuir, Freundlich, Dubinin-Radushkevich, Redlich-Peterson, and BET. The Langmuir isotherm model considers MR sorption on energetically equivalent sites of MCM-41-type silica. The saturation point is attained at monolayer formation and no further sorption can be realized as all sites are occupied by dye molecules. The Freundlich isotherm theory can be applied to the heterogeneous surface with non-equivalent adsorption sites. It is used to describe the multilayer reversible adsorption. The empirical Dubinin-Radushkevich isotherm model does not assume the homogeneity of the surface and the constancy of the sorption potential. It is widely applied to elucidate the sorption mechanism onto a heterogeneous surface. The parameters of MR equilibrium sorption determined from the linearized forms of Langmuir, Freundlich and Dubinin-Radushkevich equations are listed in Table 3.
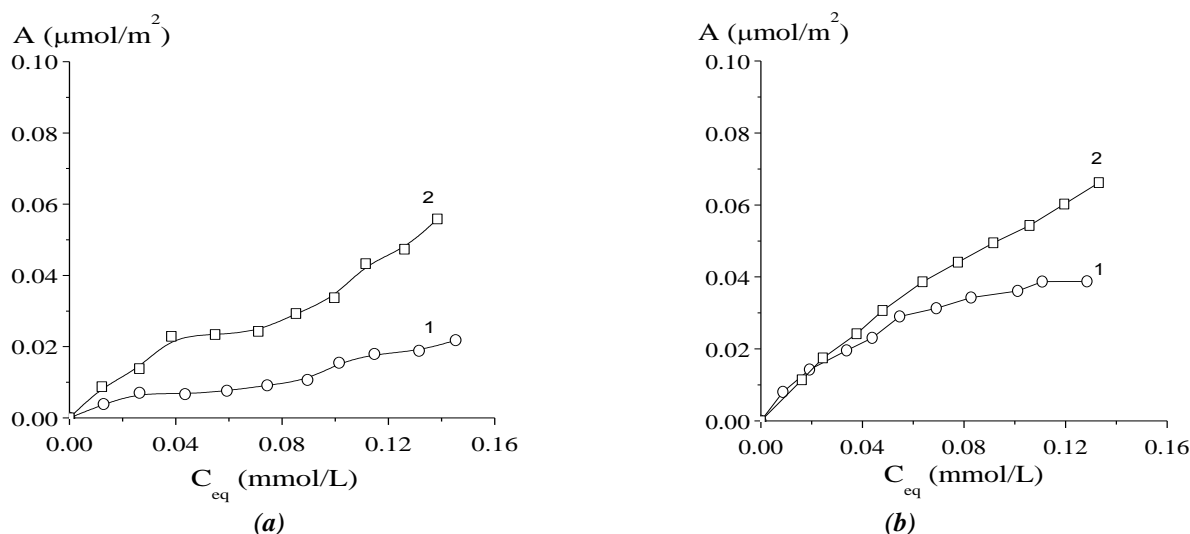
Figure 10. Isotherms of MR sorption on MCM-41 *(1)* and *β*-CD-MCM-41 *(2)* silica from phosphate buffer solutions with pH 1.0 *(a)* and pH 7.0 *(b)* at 293 K.

The Redlich-Peterson model combines the features of both Langmuir and Freundlich equations. It can predict adsorption either on heterogeneous or homogenous sites of silica surface for which the mechanism of adsorption is hybrid and does not follow ideal monolayer formation. The classical BET isotherm model describes the multilayer adsorption from the gas phase. Therefore, its direct application for liquid-solid phase process leads to erroneous results. In the present paper, the corrected form of the BET equation proposed by Ebadi *et al.* was used for modelling MR sorption on silica surface from phosphate buffer solutions [42]. Sorption parameters of Redlich-Peterson and BET equations obtained from nonlinear regression analysis are represented in Table 3.

Isotherms of MR sorption on MCM-41 surface at pH 1.0 and 7.0 attain saturation at the equilibrium dye concentration of about 0.11 mmol/L (Figure 10). Another situation is observed in the case of *β*-CD-MCM-41, when the increase of MR sorption is incomplete in the studied region of equilibrium concentrations (Figure 10). The area per MR molecule calculated by HyperChem program for the dye in flat orientation equals to 0.76 nm^2 (Figure 11).

Obviously, for monolayer formation, 2.19 µmol of MR per m^2 of silica carrier is required. At applied experimental conditions the content of dye molecules sorbed on the silica surfaces is much lower (Figure 10).
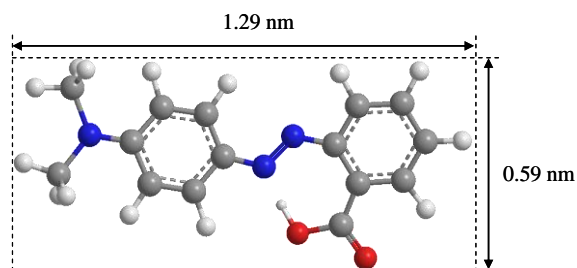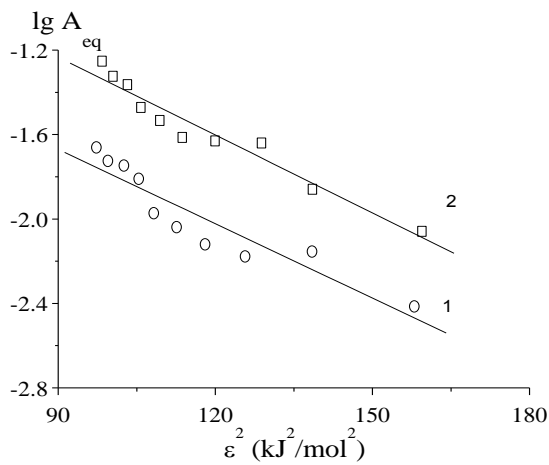

Figure 11. Geometrical parameters of methyl red molecule.

In order to determine the best-fitting model for each isotherm, values of the coefficient of determination (R^2) and the reduced Chi-square (χ^2_{red}) were evaluated and compared (Table 3). Error analysis showed that the Dubinin-Radushkevich as well as Redlich-Peterson isotherm models are the most appropriate for fitting the experimental data obtained at pH 1.0 and 7.0. The parameters obtained from linearized form of the Dubinin-Radushkevich isotherm (Figure 12) were used to calculate the mean free energy of MR sorption on MCM-41 and *β*-CD-MCM-41 samples (Table 3). Obtained results reveal that the free energy change during physical sorption of H$^+$MR protolytic forms in acidic medium is lower than in the case of anion MR$^-$ species sorption, which prevail at neutral pH.
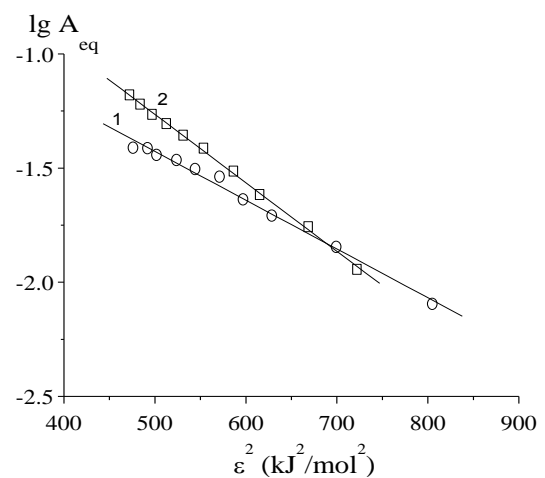
Table 3

The parameters of MR equilibrium sorption on MCM-41 and *β*-CD-MCM-41 silica calculated using Langmuir, Freundlich, Dubinin-Radushkevich, Redlich-Peterson and BET models.

Equilibrium adsorption model	Sorption parameters	MCM-41 pH 1.0	MCM-41 pH 7.0	β-CD-MCM-41 pH 1.0	β-CD-MCM-41 pH 7.0
Langmuir $A_{eq} = A_m \dfrac{K_L C_{eq}}{1 + K_L C_{eq}}$ $\dfrac{C_{eq}}{A_{eq}} = \dfrac{1}{K_L A_m} + \dfrac{C_{eq}}{A_m}$	K_L (1/µmol)	-4.117	27.801	9.520	11.097
	A_m (µmol/m^2)	-1.347	0.049	0.611	0.051
	R^2	0.001	0.903	0.002	0.621
	χ^2_{red}	0.021	0.093	0.059	0.506
Freundlich $A_{eq} = K_F C_{eq}^{1/n}$ $lg A_{eq} = lg K_F + \dfrac{1}{n} lg C_{eq}$	$K_F \cdot 10^{-3}$ (1/g)	33879	0.147	21192	0.178
	n	0.385	1.669	0.118	1.229
	R^2	0.587	0.985	0.936	0.996
	χ^2_{red}	0.060	8.4·10^{-4}	0.011	2.5·10^{-4}
Dubinin-Radushkevich $A_{eq} = (A_m) exp(-K_{DR} \varepsilon^2)$ $lg A_{eq} = lg A_m - K_{DR} \varepsilon^2$ $\varepsilon = RT ln[1 + \dfrac{1}{C_{eq}}]$ $E = (2 K_{DR})^{-0.5}$	K_{DR} (mol^2/kJ^2)	0.016	0.015	0.002	0.003
	A_m (µmol/m^2)	0.089	0.3815	0.349	1.522
	R^2	0.868	0.944	0.991	0.999
	E (J/mol)	5.590	5.774	15.811	12.909
	χ^2_{red}	0.002	5.2·10^{-4}	4.2·10^{-6}	1.5·10^{-7}
Redlich-Peterson $A_{eq} = \dfrac{K_R C_{eq}}{1 + a_R C_{eq}^B}$	$K_R \cdot 10^{-3}$ (L/m^2)	0.161	1.062	0.379	0.461
	a_R (L/mmol)	-4.373	15.075	-13.210	3.049
	B	0.391	0.892	0.687	0.642
	R^2	0.778	0.993	0.939	0.999
	χ^2_{red}	0.003	1.5·10^{-6}	9·10^{-4}	1.5·10^{-7}
BET $A_{eq} = \dfrac{A_m K_S C_{eq}}{(1 - K_L C_{eq})(1 - K_L C_{eq} + K_S C_{eq})}$	K_S (L/mmol)	0.033	15.720	0.344	10.710
	K_L (L/mmol)	41.930	1.22×10^{-12}	40.430	1.776
	A_m (µmol/m^2)	1.743	0.059	0.375	0.039
	R^2	0.796	0.991	0.942	0.996
	χ^2_{red}	0.003	1.4·10^{-6}	8.6·10^{-4}	1.3·10^{-7}

(a)   *(b)*

Figure 12. Linearized plots of the Dubinin-Radushkevich isotherms for MR sorption on MCM-41 *(1)* and *β*-CD-MCM-41 *(2)* silica from phosphate buffer solutions with pH 1.0 *(a)* and pH 7.0 *(b)* at 293 K.

Conclusions

New organosilica material was obtained by condensation of TEOS and *β*-CD-containing silane in the presence of ionic alkylammonium surfactant. IR spectral and chemical analysis of surface functional groups as well as low-temperature nitrogen adsorption-desorption isotherms, X-ray diffraction, transmission electron microscopy and dynamic light scattering were applied to estimate chemical and porous structure of the resulting material. It was found that incorporation of *β*-CD-silane into the sol-gel synthesis leads to the formation of a silica material with less distinct long-range ordering of porous structure and lower surface area compared to parent MCM-41. In order to evaluate the contribution of macrocyclic surface centres to the removal of methyl red from aqueous solutions, dye sorption was studied on parent MCM-41 and chemically modified *β*-CD-MCM-41 in phosphate buffer solutions with pH 1.0 and 7.0.

The obtained results proved that the incorporation of *β*-CD moieties into the silica structure leads to a 2-fold increase of methyl red sorption per unit of surface. Equilibrium sorption data were analyzed using widely applied isotherm models. It was found that the Dubinin-Radushkevich and Redlich-Peterson isotherm models are the most appropriate to describe sorption of methyl red on MCM-41 and *β*-CD-MCM-41 surface.

References

1. Connors, K.A. The stability of cyclodextrin complexes in solution. Chemical Reviews, 1997, 97, pp. 1325-1357.
   DOI: https://doi.org/10.1021/cr960371r.
2. Matsui, Y.; Nishioka, T.; Fujita, T. Quantitative structure-reactivety analysis of the inclusion mechanism by cyclodextrins. Topics in Current Chemistry, 1985, 128, pp. 61-89.
   DOI: https://doi.org/10.1021/tx970166m.
3. Szejtli, J. Introduction and general overview of cyclodextrin chemistry. Chemical Reviews, 1998, 98(5), pp. 1743-1754.
   DOI: 10.1021/cr970022c.
4. Gloe, K. Macrocyclic chemistry: current trends and future perspectives. Springer: Netherlands, 2005, 450 p.
   DOI: 10.1007/1-4020-3687-6.
5. Issaq, H.J. Ed. A century of separation science. CRC Press: New York, 2001, 776 p.
6. Bibby, A.; Mercier, L. Adsorption and separation of water-soluble aromatic molecules by cyclodextrin-functionalized mesoporous silica. Green Chemistry, 2003, 5(1), pp. 15-19.
   DOI: https://doi.org/10.1039/B209251B.
7. Hug, R.; Marcier, L.; Kooyman, P.J. Incorporation of cyclodextrin into mesostructured silica.

8. Liu, C.; Naismith, N.; Economy, J. Advanced mesoporous organosilica materials containing microporous *β*-cyclodextrin for the removal of humic acid from water. Journal of Chromatography A, 2004, 1036(2), pp. 113-118.
   DOI: https://doi.org/10.1016/j.chroma.2004.02.076.
9. Wang, H.C.; Li, J.T.; Lin, P.; Li, X.B.; Bian, X.B.; Wang, X.M.; Li, B.L. Low temperature strategy to synthesize high surface area mesoporous hydroxypropyl-*β*-cyclodextrin-based silica via benign template removal. Microporous and Mesoporous Materials, 2010, 134(1-3), pp. 175-180. DOI: https://doi.org/10.1016/j.micromeso.2010.05.023.
10. Phan, T.N.T.; Bacquet, M.; Laureyns, J.; Morcellet, M. New silica gels functionalized with 2-hydroxy-3-methacryloyloxypropyl-*β*-cyclodextrin using coating or grafting methods. Physical Chemistry Chemical Physics, 1999, 1(22), pp. 5189-5195.
    DOI: https://doi.org/10.1039/A905713G.
11. Roik, N.V.; Belyakova, L.A. Interaction of supramolecular centers of silica surface with aromatic amino acids. Journal of Colloid and Interface Science, 2011, 362(1), pp. 172-179.
    DOI: https://doi.org/10.1016/j.jcis.2011.05.085.
12. Shvets, O.; Belyakova, L. Synthesis, characterization and sorption properties of silica modified with some derivatives of β-cyclodextrin. Journal of Hazardous Materials, 2015, 283, pp. 643-656. DOI: https://doi.org/10.1016/j.jhazmat.2014.10.012.
13. Liu, M.; Da, S.-L.; Feng, Y.-Q.; Li, L.-S. Study on the preparation method and performance of a new β-cyclodextrin bonded silica stationary phase for liquid chromatography. Analytica Chimica Acta, 2005, 533, pp. 89-95.
    DOI: https://doi.org/10.1016/j.aca.2004.10.079.
14. Fujimura, K.; Ueda, T.; Ando, T. Retention behavior of some aromatic compounds on chemically bonded cyclodextrin silica stationary phase in liquid chromatography. Analytical Chemistry, 1983, 55(3), pp. 446-450.
    DOI: https://doi.org/10.1021/ac00254a009.
15. Kawaguchi, Y.; Tanaka, M.: Nakae, M.; Funazo, K.; Shono, T. Chemically bonded cyclodextrin stationary phases for liquid chromatographic separation of aromatic compounds. Analytical Chemistry, 1983, 55(12), pp. 1852-1857.
    DOI: https://doi.org/10.1021/ac00262a005.
16. Bai, Z.-W.; Lai, X.-H.; Chen, L.; Ching, C.-B.; Ng, S.-C. Arylcarbamoylated allylcarbamido-*β*-cyclodextrin: synthesis and immobilization on nonfunctionalized silica gel as a chiral stationary phase. Tetrahedron Letters, 2004, 45(39), pp. 7323-7326.
    DOI: https://doi.org/10.1016/j.tetlet.2004.08.007.
17. Xu, X.; Liu, Z.; Zhang, X.; Duan, S.; Xu, S.; Zhou, C. *β*-Cyclodextrin functionalized mesoporous silica for electrochemical selective sensor: Simultaneous

determination of nitrophenol isomers. Electrochimica Acta, 2011, 58, pp. 142-149. DOI: https://doi.org/10.1016/j.electacta.2011.09.015.

18. Chen, X.; Yao, X.; Wang, C.; Chen, L.; Chen, X. Mesoporous silica nanoparticles capped with fluorescence-conjugated cyclodextrin for pH-activated controlled drug delivery and imaging. Microporous and Mesoporous Materials, 2015, 217, pp. 46-53. DOI: https://doi.org/10.1016/j.micromeso.2015.06.012.

19. Roik, N.V.; Belyakova, L.A. Sol-gel synthesis of MCM-41 silicas and selective vapor-phase modification of their surface. Journal of Solid State Chemistry, 2013, 207, pp. 194-202. DOI: https://doi.org/10.1016/j.jssc.2013.09.027.

20. Staab, H.A. New Methods of Preparative Organic Chmistry IV. Syntheses using heterocyclic amides (azolides). Angewandte Chemie. International Edition in English, 1962, 1(7), pp. 351-367. DOI: https://doi.org/10.1002/anie.196203511.

21. Defreese, J.L.; Katz, A. Shape-selective covalent binding in bulk, microporous imprinted silica. Microporous and Mesoporous Materials, 2006, 89(1-3), pp. 25-32. DOI: https://doi.org/10.1016/j.micromeso.2005.09.023.

22. Li, J.; Zhu, K.; Shang, J.; Wang, D.; Nie, Z.; Guo, R.; Liu, C.; Wang, Z.; Li, X.; Liu, J. Fluorescent functionalized mesoporous silica for radioactive material extraction. Separation Science and Technology, 2012, 47, pp. 1507-1513. DOI: http://dx.doi.org/10.1080/01496395.2012.655833.

23. Katz, A.; Davis, M.E. Molecular imprinting of bulk, microporous silica. Nature, 2000, 403, pp. 286-289. DOI: http://dx.doi.org/10.1038/35002032.

24. Fryxell, G.E.; Wu, H.; Lin, Y.; Shaw, W.J.; Birnbaum, J.C.; Linehan, J.C.; Nie, Z.; Kemner, K.; Kelly, S. Lanthanide selective sorbents: self-assembled monolayers on mesoporous supports (SAMMS). Journal of Materials Chemistry, 2004, 14(22), pp. 3356-3363. DOI: http://dx.doi.org/10.1039/B408181A.

25. Roik, N.V.; Belyakova, L.A. Mesoporous silica nanoparticles equipped with surface nanovalves for pH-controlled liberation of doxorubicin. Interface Focus, 2016, 6(6), pp. 1-10. DOI: http://dx.doi.org/10.1098/rsfs.2016.0041.

26. Trofymchuk, I.M.; Roik, N.V.; Belyakova, L.A. Structural variety and adsorptive properties of mesoporous silicas with immobilized oligosaccharide groups. Nanoscale Research Letters, 2017, 12, pp. 307-320. DOI: http://dx.doi.org/10.1186/s11671-017-2072-2.

27. Bragg, W.L. The diffraction of short electromagnetic waves by a crystal. Proceedings of the Cambridge Philosophical Society, 1913, 17, pp. 43-57.

28. Fenelonov, V.B.; Romannikov, V.N.; Derevyankin, A.Yu. Mesopore size and surface area calculations for hexagonal mesophases (types MCM-41, FSM-16, *etc.*) using low-angle XRD and adsorption data. Microporous and Mesoporous Materials, 1999, 28, pp. 57-72. DOI: https://doi.org/10.1016/S1387-1811(98)00280-7.

29. Korenman, I.M. Photometric analysis. Methods of determination of organic compounds. Khimia: Moscow, 1970, 343 p. (in Russian).

30. Belyakova, L.A.; Besarab, L.N.; Roik, N.V.; Lyashenko, D.Yu.; Vlasova, N.N.; Golovkova, L.P.; Chuiko, A.A. Designing of the centers for adsorption of bile acids on a silica surface. Journal of Colloid and Interface Science, 2006, 294, pp. 11-20. DOI: https://doi.org/10.1016/j.jcis.2005.06.081.

31. Nakanishi, K. Infrared absorption spectroscopy–practical. Holden-Day, Inc.: San Francisco and Nankodo Company Ltd.: Tokyo, 1962, 233 p.

32. Brunauer, S.; Emmet, P.H.; Teller, E. Adsorption of gases in multimolecular layers. Journal of American Chemical Society, 1938, 60, pp. 309-319. DOI: https://doi.org/10.1021/ja01269a023.

33. Lee, C.-K.; Liu, S.-S.; Juang, L.-C.; Wang, C.-C.; Lin, K.-S.; Lyu, M.-D. Application of MCM-41 for dyes removal from wastewater. Journal of Hazardous Materials, 2007, 147, pp. 997-1005. DOI: https://doi.org/10.1016/j.jhazmat.2007.01.130.

34. Kachbouri, S.; Mnasri, N.; Elaloui, E.; Moussaoui, Y. Tuning particle morphology of mesoporous silica nanoparticles for adsorption of dyes from aqueous solution. Journal of Saudi Chemical Society. DOI: https://doi.org/10.1016/j.jscs.2017.08.005.

35. Kang, J.-K.; Park, J.-A.; Kim, J.-H.; Lee, C.-G.; Kim, S-B. Surface functionalization of mesoporous silica MCM-41 with 3-aminopropyltrimethoxy silane for dye removal: kinetic, equilibrium, and thermodynamic studies. Desalination and Water Treatment, 2016, 57, pp. 7066-7078. DOI: http://dx.doi.org/10.1080/19443994.2015.1014856.

36. Wu, Y.; Zhang, M.; Zhao, H.; Yang, S.; Arkin, A. Functionalized mesoporous silica material and anionic dye adsorption: MCM-41 incorporated with amine groups for competitive adsorption of Acid Fuchsine and Acid Orange II. RSC Advances, 2014, 4(106), pp. 61256-61267. DOI: http://dx.doi.org/ 10.1039/C4RA11737A.

37. Torabinejad, A.; Nasirizadeh, N.; Yazdanshenas, M.E.; Tayebi, H.A. Synthesis of conductive polymer-coated mesoporous MCM-41 for textile dye removal from aqueous media. Journal of Nanostructure in Chemistry, 2017, 7, pp. 217-229. DOI: https://doi.org/10.1007/s40097-017-0232-7.

38. Torabinejad, A.; Nasirizadeh, N.; Yazdanshenas, M.E.; Tayebi, H.A. Synthesize and characterization of Aminosilane functionalized MCM-41 for removal of anionic dye: Kinetic and thermodynamic study, International Journal of Nano Dimension, 2016, 7(4), pp. 295-307. DOI: https://doi.org/10.7508/ijnd.2016.04.005.

39. Tawarah, K.M.; Abu-Shamleh, H.M. A spectrophotometric study of the acid-base equilibria of *o*-methyl red in aqueous solutions. Dyes and

Pigments, 1991, 17(13), pp. 203-215. DOI: https://doi.org/10.1016/0143-7208(91)80027-7.

40. Kolthoff, I.M. Acid-base indicators. 2nd pr., transl. by Rosenblum C. The Macmillan Company: New York, 1953, 414 p.

41. Tobey, S.W. The acid dissociation constant of methyl red. A spectrophotometric measurement. Journal of Chemical Education, 1958, 35(10), pp. 514-515.

DOI: https://doi.org/10.1021/ed035p514.

42. Ebadi, A.; Mohammadzadeh, J.S.S.; Khudiev, A. What is the correct form of BET isotherm for modelling liquid phase adsorption? Adsorption, 2009, 15(1), pp. 65-73.
DOI: https://doi.org/10.1007/s10450-009-9151-3.